using Newton's method and the resulting linear system for the five unknowns, f,u,v,w, and s can be solved by the block-elimination method discussed in Ref. 5.

Results and Discussion

Results are obtained for two separate flows consisting of a zero pressure gradient and an adverse pressure gradient. Calculations are done for three different linearization schemes. The first one is the usual procedure in which the b term in Eq. (12c) is assumed to be known from a previous iteration, the second one is to neglect the variation of f''_w in the eddy-viscosity formulas ($s\equiv 0$) and assume it to be known from a previous iteration. In the latter case we have four unknowns (f,u,v, and w), in contrast to the third linearization scheme in which we have five unknowns (f,u,v,w, and s), as described in the previous section, and all the terms in the equations are linearized fully by Newton's method.

Figure 1a shows the rate of convergence of the three linearization schemes for the case of a zero pressure-gradient flow. The calculations were started as laminar for a unit Reynolds number of 10^6/ft at the leading edge of the plate; the transition was specified very close to the leading edge and approximately eight x stations were taken in the region $0<x<1$. Between $x=1$ and $x=10$, two different Δx spacings corresponding to $\Delta x=0.25$ and 1 were used. From the results shown in Fig. 1a, we see the rate of convergence with the full Newton (scheme 3, system with five unknowns) is quadratic in all cases and that, with three iterations, the error term in the wall shear parameter f''_w is reduced from 10^0, 10^{-3} to 10^{-6}. The rate of convergence of the system with four unknowns (scheme 2), on the other hand, is linear. Thus, with both schemes one can specify a small tolerance error ($\equiv 10^{-6}$) and the corresponding results obtained. In contrast, the usual linearization procedure (scheme 1) produces oscillations, restricts the tolerance error that can be specified, and will lead to significantly large computer times if a small convergence criterion is specified.

The computation times of the three linearization schemes, if in each case the calculations are allowed to continue for, say, eight iterations in a given x station, are 0.040, 0.043, and 0.050 min for schemes 1-3, respectively. The computer time associated with scheme 3 is only 20% more than that of scheme 1 because the added Eqs. (15) contribute little to the general A matrix used in the block-elimination method.[5] Of course, the slight increase of computer time associated with scheme 3 can be overcome easily by noting that scheme 3 takes two iterations to achieve a tolerance error of 10^{-3} while scheme 1 takes up to approximately six iterations. This gain increases as the tolerance is decreased.

Figure 1b shows the rate of convergence of the three linearization schemes for a flow with pressure gradient and depicts the same results and conclusions indicated for the zero pressure gradient flow. They show that the rate of convergence is quadratic when Newton's method is applied in full to the momentum equation, and very small values of convergence criterion can be specified without oscillation. The new linearization scheme should lead to substantial savings in computer time in interactive calculations.

Acknowledgment

This research was supported under the National Science Foundation Grant MEA-8018565.

References

[1] Cebeci, T. and Smith, A. M. O., *Analysis of Turbulent Boundary Layers,* Academic Press, New York, 1974.

[2] Cebeci, T., "Separated Flows and Their Representation by Boundary-Layer Equations," California State University, Long Beach, Mech. Eng. Rept. ONR-CR215-234-2, 1976.

[3] Crank, J. and Nicolson, P., "A Practical Method for Numerical Evaluation of Solutions of Partial Differential Equations of the Heat-Conduction Type," *Proceedings of Cambridge Phil. Soc.*, Vol. 43, 50, 1947.

[4] Keller, H. B., "A New Difference Scheme for Parabolic Problems," *Numerical Solution of Partial-Differential Equations,* edited by J. Bramble, Vol. II, Academic Press, New York, 1970.

[5] Bradshaw, P., Cebeci, T., and Whitelaw, J. H., *Engineering Calculation Methods of Turbulent Flows,* Academic Press, London, 1981.

Effect of Angle of Attack on Rotor Trailing-Edge Noise

S.-T. Chou* and A. R. George†
Cornell University, Ithaca, New York

BOUNDARY-LAYER trailing-edge noise has been identified as an important rotor broadband noise mechanism in many cases, especially at high frequencies for large rotors when inflow turbulence is weak.[1] Previous analyses of this noise mechanism used zero blade angle of attack for input data. In practice, to produce desired loadings, rotor blades are operated at various angles of attack. This Note, which is a follow-up to an earlier paper by Kim and George,[2] examines the important effect of change of blade's angle of attack on rotor trailing-edge noise.

Using the same model and assumptions, the general result for the far-field sound pressure level radiated by the turbulent boundary layer passing the rotor blades' trailing edges can be directly adapted from Ref. 2 as

$$\langle S_l(x,f)\rangle = \frac{Bf^2b^2U_c^2\sin^2\phi}{2\pi\rho c_0^3r^2}\sum_{n=-\infty}^{n=\infty}\frac{F_g(|f-n\Omega|)S_{pp}(|f-n\Omega|)}{(f-n\Omega)^2(1+b/\ell_2(|f-n\Omega|))}\times J_n^2\left(\frac{f}{\Omega}M_0\cos\phi\right) \tag{1}$$

where

b = blade span
B = number of blades
c_0 = the undisturbed sound speed
$c_l - is_l = E^*[2\mu(1+M)]$
$c_2 - is_2 = E^*[2(\mu+\mu M+K_l)]$
f = acoustic frequency, Hz
$F_g = F^2+G^2$

$$F = \left(\frac{\mu+M\mu+K_l}{\mu+M\mu}\right)^{1/2}\{(c_l+s_l)\cos 2K_l + (c_l-s_l)\sin 2K_l\} + 1-(c_2+s_2)$$

$$G = \left(\frac{\mu+M\mu+K_l}{\mu+M_\mu}\right)^{1/2}\{(c_l-s_l)\cos 2K_l - (c_l+s_l)\sin 2K_l\} - (c_2-s_2)$$

Received Jan. 12, 1984; revision received Feb. 22, 1984.

*Graduate Research Assistant, Sibley School of Mechanical and Aerospace Engineering. Student Member AIAA.

†Professor and Director, Sibley School of Mechanical and Aerospace Engineering. Associate Fellow AIAA.

$K_1 = \dfrac{\omega c}{2U_c}, \quad \mu = \dfrac{Mk}{\beta^2}$

$\ell_2(|f-n\Omega|) \simeq 2.1\dfrac{U_c}{2\pi|f-n\Omega|}$

r = distance from rotor hub to observer

$S_{pp}(|f-n\Omega|) = \left(\dfrac{1}{2}\rho U^2\right)^2\left(\dfrac{\delta^*}{U}\right)S_0(\bar{\omega}), \quad \bar{\omega} \equiv \dfrac{2\pi|f-n\Omega|\delta^*}{U}$

U_c = turbulence convection velocity
ρ = density of the acoustic media
ϕ = elevation angle of observer from the rotor plane

As the blade's angle of attack and Mach number are changed, the characteristics of the turbulent boundary layer over the rotor change, resulting in a change of δ^*, the displacement thickness. Previous studies used the flat plate boundary-layer theory to calculate δ^* and used it as an input to the analysis. However, as pointed out by Schlinker and Amiet,[3] the flat plate boundary-layer theory cannot predict δ^* except approximately for the zero lift case. They measured the boundary-layer thickness for a NACA 0012 airfoil section of 0.41 m chord, as the Mach number ranged from 0.15 to 0.5 and the angle of attack changed from -0.4 to 12 deg. Theoretically, both Reynolds number and Mach number affect δ^*. With increasing Reynolds number, δ^* decreased slowly with $Re^{-1/5}$; with increasing Mach number, the compressibility effect tends to increase δ^*. In fact, these two effects essentially cancelled each other, thus explaining the fact that their data showed a very weak variation with Mach number or Reynolds number, which suggested a simple correlation of δ^* with α, the angle of attack alone. Note that the data were measured for boundary-layer thickness δ, while in Eq. (1) the surface pressure spectrum S_{pp} was characterized by the displacement thickness δ^*. Thus, by using the well-known one-seventh power law, δ was transformed to δ^*. Then, a curve fitting technique led to the following empirical expression:

$$\delta^*/c = (24.3 + 0.6625\alpha) \times 10^{-4} \tag{2a}$$

for $\alpha < 4$ deg and

$$\delta^*/c = (26.95 + 0.6625\beta + 0.3044\beta^2 + 0.0104\beta^3) \times 10^{-4} \tag{2b}$$

for $\alpha \geq 4$ deg, where $\beta = \alpha - 4$ deg, and α and β are in degrees. This curve and the data are shown in Fig. 1. Due to very limited data available, no correlations are made to Reynolds number and Mach number. This limits the application of the preceding equations to Reynolds number between 9.5×10^5 and 5.2×10^6.

Next we examine S_{pp}, the incident surface pressure spectral density. As can be seen in Eq. (1), the term that is still left undetermined is $S_0(\bar{\omega})$. Empirical expressions for $S_0(\bar{\omega})$ can be obtained from experiments. In this study, two sets of experiments were used, one by Yu and Joshi[4] and one by Brooks and Hodgson.[5] Their data seem to agree well, and again curve fitting leads to the following expression:

$$S_0(\bar{\omega}) = 1.732 \times 10^{-3}\bar{\omega}/(1 - 5.489\bar{\omega} + 36.74\bar{\omega}^2 + 0.1505\bar{\omega}^5) \tag{3a}$$

for $\bar{\omega} < 0.06$, where $\bar{\omega} = 2\pi f\delta^*/U$, and

$$S_0(\bar{\omega} = 1.4216 \times 10^{-3}\bar{\omega}/(0.3261 + 4.1837\bar{\omega} + 22.818\bar{\omega}^2 + 0.0013\bar{\omega}^3 + 0.0028\bar{\omega}^5) \tag{3b}$$

for $0.06 \leq \bar{\omega} \leq 20$. Figure 2 shows the plot of $S_0(\bar{\omega})$ vs $\bar{\omega}$ along with the experimental data and the flat plate result.

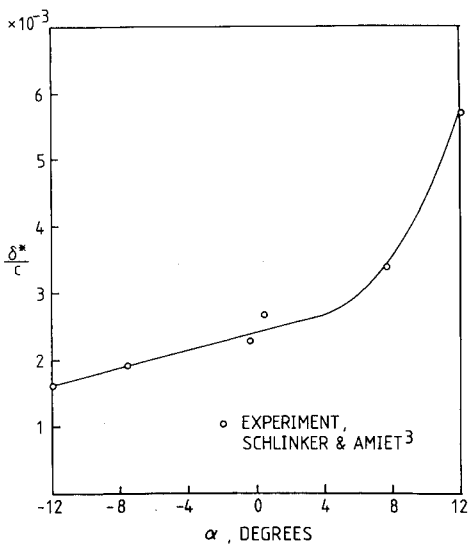

Fig. 1 Variation of δ^* with α.

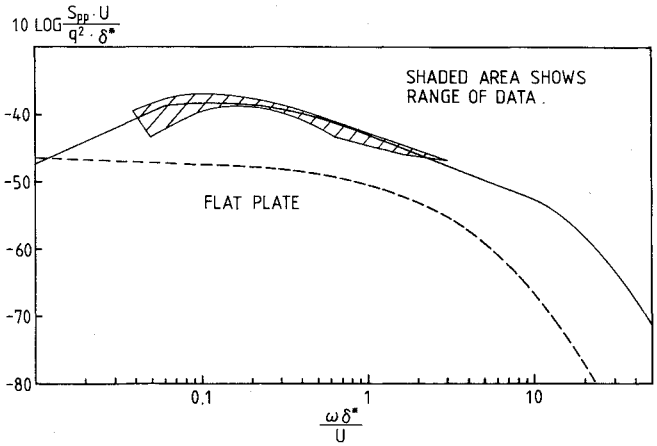

Fig. 2 Plots of $S_0(\bar{\omega})$ vs $\bar{\omega}$.

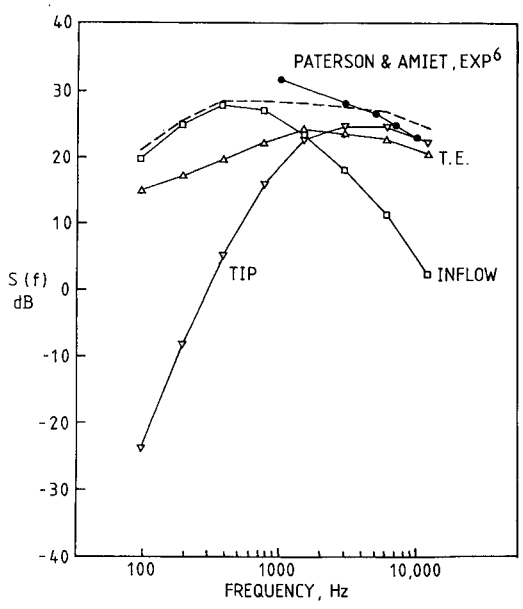

Fig. 3 Comparison of predictions for model rotor, experiment of Paterson and Amiet,[6] no grid, test VA-C-1.

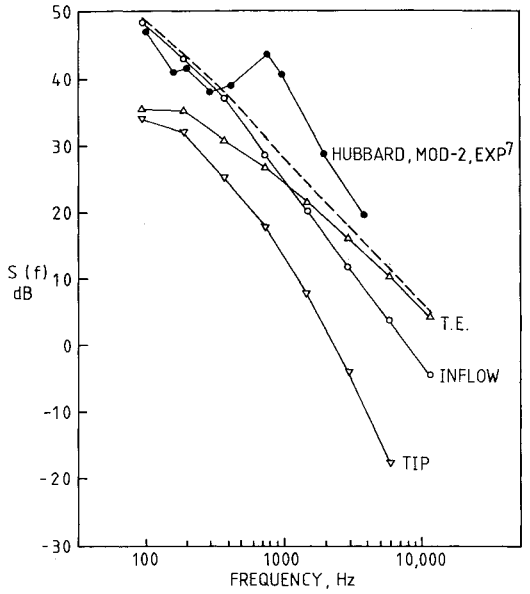

Fig. 4 Comparison of predictions with Hubbard et al.'s experiment[7] for MOD-2 wind turbine, $\Lambda = 55$ m, $\sqrt{w^2} = 1$ m/s, ground distance = 69 m.

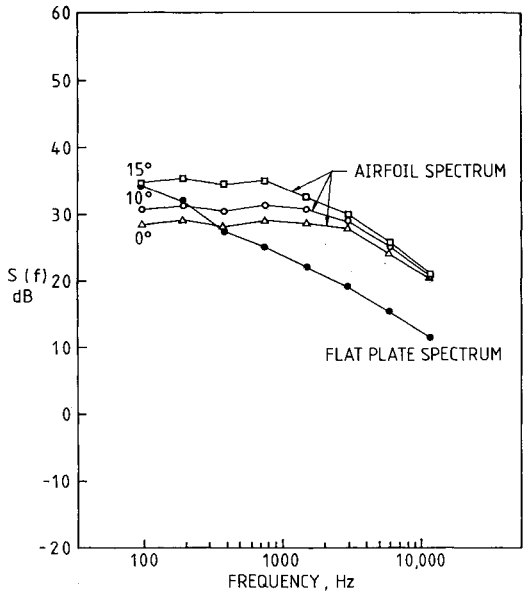

Fig. 5 Effect of rotor pitch on trailing-edge noise, UH-1, $\phi = -27$ deg.

Boundary-layer trailing-edge noise is not the only source of rotor broadband noise. Other mechanisms such as inflow turbulence and tip vortex separation also contribute significantly to the noise radiation. Thus, to evaluate the present analysis by comparing with existing experiments, one must also include other possible sources. As discussed in Ref. 1, trailing-edge noise can be important for low inflow turbulence levels or when considering a large rotor. The first experiment for comparison is an indoor model rotor test performed at the UTRC anechoic wind tunnel by Paterson and Amiet.[6] The case we picked corresponded to the no-grid case which had the lowest inflow turbulence level. Figure 3 shows the comparison. Trailing-edge noise, in this case, does not seem to be dominant in the frequency range of interest; however, it is significant and when we add up all the contributions, the result agrees very well with the experiment. The second comparison is to the MOD-2 wind turbine generator noise data of Hubbard and Shepherd.[7] Figure 4 shows the result; in this case, trailing-edge noise dominates for frequencies higher than about 1000 Hz.

Figure 5 shows the effect of angle of attack on the trailing-edge noise for a UH-1 helicopter. The result leads to a conclusion that the primary effect of angle of attack is in the low- to mid-frequency range, where the noise level increases with angle of attack. However, in the high-frequency range, the change of noise level due to change of angle of attack is not very significant. The comparison of predictions using the present analysis to that using flat plate data only[2] shows the important effect of the angle of attack on rotor trailing-edge noise.

Additional examples are given in Ref. 8.

Acknowledgments

This research was supported by NASA Langley Research Center, Dr. F. Farassat, Technical Monitor.

References

[1] George, A. R. and Chou, S.-T., "Comparison of Broadband Noise Mechanisms, Analyses, and Experiments on Rotors," *Journal of Aircraft*, Vol. 21, Aug. 1984, pp. 583-592; also AIAA Paper 83-0690, April 1983.

[2] Kim, Y. N. and George, A. R., "Trailing-Edge Noise from Hovering Rotors," American Helicopter Society Preprint 80-60; also *AIAA Journal*, Vol. 20, Sept. 1982, pp. 1167-1174.

[3] Schlinker, R. H. and Amiet, R. K., "Helicopter Rotor Trailing Edge Noise," NASA CR-3470, Nov. 1981.

[4] Yu, J. C. and Joshi, M. C., "On Sound Radiation from the Trailing Edge of an Isolated Airfoil in a Uniform Flow," AIAA Paper 79-0603, March 1979.

[5] Brooks, T. F. and Hodgson, T. H., "Prediction and Comparison of Trailing Edge Noise Using Measured Surface Pressures," AIAA Paper 80-0977, June 1980.

[6] Paterson, R. W. and Amiet, R. K., "Noise of a Model Helicopter Rotor Due to Ingestion of Turbulence," NASA CR-3213, Nov. 1979.

[7] Hubbard, H. H., Shepherd, K. P., and Grosveld, F. W., "Sound Measurements of the MOD-2 Wind Turbine Generator," NASA CR-165752, July 1981.

[8] George, A. R. and Chou, S.-T., "Broadband Rotor Noise Analysis," NASA CR-3797, April 1984.

Thermal Performance of a Logarithmic-Spiral Resonance Tube

Rafik A. Neemeh,* P. Perry Ostrowski,† and James H.T. Wu‡
Concordia University, Montreal, Canada

Introduction

THE simple Hartmann-Sprenger tube consists of a closed-end tube that is excited by an underexpanded gas jet facing its open end to produce violent, cyclic fluid oscillations internally and externally. Although this phenomenon has been known for some time, the heat generation capability of this device has been exploited only relatively recently.[1] Sprenger experimented to demonstrate that end-wall tem-

Received Dec. 12, 1983; revision received Jan. 27, 1984.

*Associate Professor, Department of Mechanical Engineering. Member AIAA.

†Research Associate, Department of Mechanical Engineering.

‡Distinguished Research Associate, Department of Mechanical Engineering. Member AIAA.